Model Predictive Control for Switching Gain Adaptation in a Sliding Mode Controller of a DC Drive with Nonlinear Friction

Benedikt Haus, Jan Hendrik Röhl, Paolo Mercorelli
Institute of Product and Process Innovation
Leuphana University of Lüneburg
Volgershall 1, 21339 Lüneburg, Germany
{haus,mercorelli}@leuphana.de,
jan.h.roehl@stud.leuphana.de

Harald Aschemann
Chair of Mechatronics
University of Rostock
Rostock, Germany
Harald.Aschemann@uni-rostock.de

***Abstract*—This paper presents an optimal, robust, adaptive tuning strategy based on a linear model predictive control (LMPC) scheme for the switching gain of a sliding mode control (SMC). The LMPC employs a moving horizon, where the dynamics of the sliding-mode-controlled system is addressed. The control design is presented exemplary for a DC drive which is subject to both nonlinear friction as well as model uncertainty. The overall control has a cascade structure. In the inner control loop for the currents, a flatness-based control is used. The outer control loop involves an integral sliding mode control of the angular velocity that is combined with a LMPC that adapts the switching height of the discontinuous control action.**

***Index Terms*—Model Predictive Control, Sliding Mode Control, Adaptive Control, Flatness, Friction Compensation, DC Drives**

I. Introduction and motivation

As an important mechatronic component, electromagnetic actuators are used in many technical applications, in particular in the automotive industry and in industrial production systems. In production systems, they play a main role in motion control and precise positioning. Mechanical, pneumatic or hydraulic components have been replaced by electromagnetic actuators due to their high efficiency, excellent dynamic behavior and cleanliness. This paper considers a direct current (DC) drive system that is subject to both nonlinear friction and model uncertainty. A combination of sliding mode control (SMC) and linear model predictive control (LMPC) is proposed for its control. Here, the LMPC adapts the switching height of the discontinuous control part and, thereby, reduces the undesired chattering effect. MPC still constitutes a developing research field in the context of machines and drives, though many applications already use such control strategies, e.g., in [1] for a PMSM or in [2] and in [3] for a DC drive. The MPC approach takes into account model-based predictions and determines the control inputs by minimizing a cost function. However, compared to classical controllers like PID, this method from the field of optimal control requires a relatively high modeling accuracy in order to yield acceptable results. SMC, however, is famous for being robust against disturbances, model mismatch and parametric uncertainties. While belonging perhaps to the most robust and versatile control strategies, SMC tends to suffer from high energy consumption and high-frequency oscillations in system inputs, states or even outputs, which certainly is to be avoided in tracking problems. To this day, many remedies have been proposed and successfully realized to deal with these problems. A very important one is the so-called boundary layer approach, see [4], by introducing a permissible region around the sliding surface, characterized by its thickness, in which no switching of the control input takes place. There are also approaches to achieve an intelligent adaptivity of switching amplitudes, of which the contribution at hand treats one. In the context of drives, SMC has even been used to *reduce* torque ripple [5], [6]. Other examples include [7], where an adaptive-gain SMC technique is employed for a brushless DC motor. The combination of SMC and LMPC allows for exploitation of the advantages of both worlds, gaining both robustness and a degree of optimality w.r.t. the specific cost function – at the cost of high control design, implementation and computation effort. Nevertheless, thanks to modern computers and micro-controllers, it is possible to go even further by using observer-based control, utilizing only a minimal number of sensors, see [8] and [9]. The goal of this contribution is to conceive a SMC with optimal adaptivity that can be implemented as simply as possible. Its effectiveness is demonstrated in simulations, subject to realistic conditions regarding disturbances and uncertainties, controlling the speed of a DC drive which was modeled with nonlinear friction. The non-linearity is represented by the Coulomb friction model, which is a classical friction model based on experiments. An extended survey of friction modeling was presented in [10] including a large number of literature references. Recent contributions mark progress in terms of identification of friction phenomena and their compensation [11]. The proposed SMC does not utilize a constant switching gain, but an adaptive gain provided by the LMPC. While technically violating Lyapunov's condition for asymptotic stability, which anyway constitutes not a necessary but only a sufficient condition,

978-1-5386-4444-7/18/$31.00 ©2018 IEEE

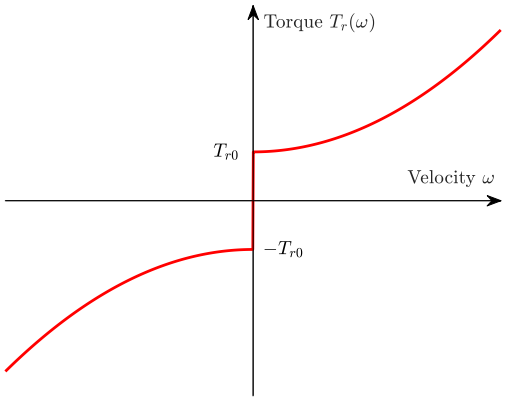

Fig. 1. Nonlinear friction torque involving Coulomb friction and a quadratic term w.r.t. the motor angular velocity.

tracking control is achieved despite simulated implementation errors, noise and load torques. The conceptual structure of the control strategy is presented in Fig. 2. The paper is organized in the following way: Section II describes the model of the DC drive with its friction nonlinearity. In Section III, the flatness-based control of the motor current is discussed, which represents the inner control loop of a cascade control structure. The design of the outer control loop is presented in the subsequent sections: Section IV describes the nonlinear sliding mode control design that involves a continuous and a discontinuous control action. The linear model-predictive control for the adaptation of the discontinuous part is discussed in Section V, Corresponding simulation results are presented in Section VI. Finally, conclusions close the paper in Section VII.

II. System Model

Though being more and more superseded by brushless drives, brushed DC motors are still significantly present in various industrial facilities and generally used in the plastics, rubber, paper, textile, printing, oil, chemical, metal, and mining industries.

A. Dynamic system modeling using ODEs

Let's consider the following system model of a DC drive

$$\frac{di(t)}{dt} = \frac{1}{L}\left(u(t) - Ri(t) - K_T\omega(t)\right) \tag{1}$$

$$\frac{d\omega(t)}{dt} = \frac{1}{J}\left(K_T i(t) - T_r(\omega(t)) - d(t)\right), \tag{2}$$

with the nonlinear friction torque

$$T_r(\omega(t)) = \left(K_f\omega^2(t) + T_{r0}\right)\operatorname{sign}(\omega(t)), \tag{3}$$

where $K_f > 0$ is a coefficient related to the quadratic term in the motor angular velocity, and T_{r0} describes the Coulomb friction part. Moreover, a lumped disturbance torque $d(t)$ represents any further external loads torques, unmodeled dynamic effects and model uncertainty. The nonlinear friction torque $T_r(\omega) = T_r(\omega(t))$ is depicted in Fig. 1.

B. Flatness of the system model

A system is differentially flat if a set of outputs, where the number of outputs is identical to the number of control inputs, can be found such that all states and inputs can be expressed in terms of those outputs (and their derivatives) [12]. A system described by the state vector $\mathbf{x} \in \mathbb{R}^n$ and the vector of control inputs $\mathbf{u} \in \mathbb{R}^m$ is denoted differentially flat if the outputs $\mathbf{y} \in \mathbb{R}^m$ have the following form

$$\mathbf{y} = \mathbf{y}(\mathbf{x}, \mathbf{u}, \dot{\mathbf{u}}, \ldots, \mathbf{u}^{(\varphi)}) \tag{4}$$

and both the states and inputs can be parametrized as

$$\mathbf{x} = \mathbf{x}(\mathbf{y}, \dot{\mathbf{y}}, \ldots, \mathbf{y}^{(\alpha)}), \quad \mathbf{u} = \mathbf{u}(\mathbf{y}, \dot{\mathbf{y}}, \ldots, \mathbf{y}^{(\gamma)}). \tag{5}$$

The flatness property is particularly attractive when explicit trajectory tracking is envisaged [13], [14]. The flat output uniquely determines the behavior of the flat system and allows for a trajectory planning in the output space. Afterwards, the output trajectories are mapped to the appropriate inputs. Concerning the determination of the flat output, only for a limited number of system types algorithms are forthcoming. Nevertheless, often an educated guess or the investigation of the output of interest – by means of the definition given by (4) and (5) – directly leads to the flat output.

III. Design of the Flatness-Based Feedforward Current Control

The model of the current dynamics (1) is obviously differentially flat. Therefore, this differential equation can be solved for the corresponding armature voltage as control input. Doing so, yields the inverse dynamics

$$u(t) = L\frac{di(t)}{dt} + Ri(t) + K_T\omega(t). \tag{6}$$

As no current measurement is available, the flatness-based control is implemented in a feedforward manner as follows

$$u(t) = L\frac{di_d(t)}{dt} + Ri_d(t) + K_T\omega(t), \tag{7}$$

with the measured velocity $\omega(t)$, the desired current $i_d(t)$ and its derivative, which is obtained by an approximate differentiation, i.e., a first-order high pass filter with corner frequency f_c

$$G(s) = \frac{2\pi f_c s}{s + 2\pi f_c}. \tag{8}$$

Note that f_c is an important tuning parameter in the case of switchings in the desired flat output signal $i_d(t)$.

IV. Design of an SMC to obtain a Globally Asymptotically Stable Control Loop

For the SMC design, consider an integral sliding surface with integral gain α and velocity error $e(t) := \omega_d(t) - \omega(t)$:

$$s(t) = e(t) + \alpha\int_0^t e(\tau)d\tau - e(0), \tag{9}$$

where $e(0)$ is the initial error, whose presence in $s(t)$ can theoretically eliminate the reaching phase ($s(0) = 0$), see [15].

In this contribution, $e(0)$ is assumed to be unknown and is set to zero in the implementation. Considering the quadratic Lyapunov function candidate

$$V(s) = \frac{1}{2}s^2(t), \tag{10}$$

its time derivative follows as

$$\begin{aligned}\dot{V} &= s(t)\dot{s}(t) \qquad (11)\\ &= s(t)\Big(\dot{\omega}_d(t) - \dot{\omega}(t) + \alpha\ (\omega_d(t) - \omega(t))\Big)\\ &= s(t)\Big(\dot{\omega}_d(t) - \frac{K_T}{J}i(t) + \frac{T_r(\omega)}{J} + \frac{1}{J}d(t) + \alpha e(t)\Big),\end{aligned}$$

the following SMC law is proposed

$$\begin{aligned}i_d(t) = &\underbrace{\frac{J}{K_T}\Big(\dot{\omega}_d(t) + \frac{T_r(\omega)}{J} + \alpha e(t)\Big)}_{i_{d_{eq}}(t)}\\ &+ \underbrace{\frac{J}{K_T}\beta\ \text{sign}(s(t))}_{i_{d_{sw}}(t)}.\end{aligned} \tag{12}$$

It should be noticed that $i_{d_{eq}}(t)$ represents the equivalent control part of the control law, and $i_{d_{sw}}(t)$ is the discontinuous control part. If the model parameters were exactly known, no external disturbance occurred, i.e. $d(t) = 0$, and a perfect cancellation was assumed, then the time derivative of the Lyapunov function (10) would result in

$$\dot{V} = -\beta|s(t)|. \tag{13}$$

Given a positive switching height $\beta > 0$, the SMC law in (12) is such that $s^2(t)$ represents a Lyapunov function of the closed loop system, see page 282 of [15].

Remark 1: Please recall that a system $\dot{x}(t) = f(x(t), u(t))$ under time-varying feedback $u(x(t), t)$ represents a non-autonomous system. This is needed, for instance, in the typical case in which $x(t)$ should exactly track a time-varying trajectory. Nevertheless, invoking the Lyapunov-like Lemma on the non-autonomous systems, the control law (12) guarantees global uniform asymptotic stability of the controlled system around the desired trajectories $\omega_d(t)$, see p. 125 of [15].

Remark 2: In real applications, however, due to parametric uncertainty in the system model, non-exact cancellations have to be considered. As a result, the following condition for the switching height must be guaranteed

$$\beta > \delta > \max|\Delta(t)|, \tag{14}$$

where it is assumed that $\Delta(t)$ is bounded by a known real quantity δ

$$\max|\Delta(t)| = \max\frac{|d(t)|}{J} + \max|\Delta_p(t)| < \delta, \tag{15}$$

where term $\max|\Delta_p(t)|$ represents the upper bound of the "residual" error cancellation due to possible parameter uncertainties after the introduction of the equivalent current $i_{d_{eq}}(t)$.

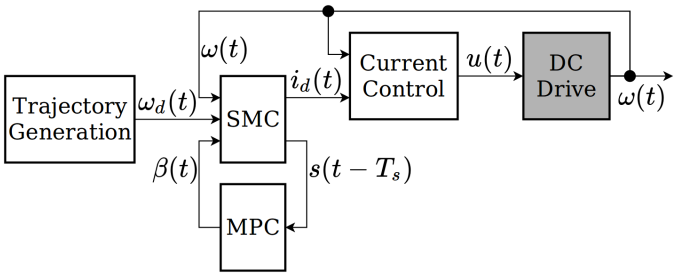

Fig. 2. Control scheme: Combination of MPC, SMC and flatness-based current control. The gray block represents the physical system. $s(t)$ must be delayed by one time step to avoid algebraic loops.

After inserting the control law into the system dynamics, the closed-loop system dynamics becomes

$$\begin{aligned}&\dot{\omega}(t) = \dot{\omega}_d(t) + \alpha\ (\omega_d(t) - \omega(t)) + \beta\text{sign}(s(t)) \qquad (16)\\ &\Rightarrow 0 = \underbrace{\dot{\omega}_d(t) - \dot{\omega}(t) + \alpha\ (\omega_d(t) - \omega(t))}_{\dot{s}(t)} + \beta\text{sign}(s(t))\\ &\Rightarrow \dot{s}(t) = -\beta\text{sign}(s(t)). \qquad (17)\end{aligned}$$

Equation (17) states the "error" dynamics, or to be more exact, the dynamics of the sliding surface of the closed-loop system.

V. LMPC FOR THE SWITCHING GAIN ADAPTATION

When designing an SMC in practice, the switching gain parameter β is often tuned only once, in a way that satisfies a condition like (14) while keeping β as small as possible. This rather conservative controller design may lead to chattering in the control input, or even in the system states or outputs. A popular mitigation technique is to introduce a permissible region (called boundary layer) with a certain thickness around the sliding surface, in which we may remain without further switchings – and, in general, without necessarily reaching or staying on the sliding surface. While this strategy has many advantages, it clashes with the basic idea of the *sliding mode* control. In this contribution, an alternative technique is proposed that consists of an MPC scheme to adaptively tune the switching height $\beta = \beta(k)$. From (17), using an explicit Euler discretization with a sampling time of $t_S = 10\ \mu s$, $t = kt_S, k = 0, 1, 2, ...$, the following discrete-time state-space representation is obtained:

$$\begin{aligned}&s(k+1) = s(k) - T_s\beta(k)\text{sign}(s(k)), \quad \text{satisfying} \qquad (18)\\ &s(k+1) = \mathbf{A}_k s(k) + \mathbf{B}_k\beta(k), \quad y(k+1) = \mathbf{C}_k s(k+1),\\ &\quad \Rightarrow \mathbf{A}_k = \mathbf{A} = 1,\ \mathbf{B}_k = -T_s\text{sign}(s(k)),\\ &\qquad \mathbf{C}_k = \mathbf{C} = 1.\end{aligned}$$

Using iterations, the system behavior can be predicted as

$$\begin{aligned}\hat{y}(k+1) &= \mathbf{C}\ \mathbf{A}\ \mathbf{x}(k) + \mathbf{C}\ \mathbf{B}_k\ u_{MPC}(k) \\ \hat{y}(k+2) &= \mathbf{C}\ \mathbf{A}^2\ \mathbf{x}(k) + \mathbf{C}\ \mathbf{A}\ \mathbf{B}_k\ u_{MPC}(k) \\ &\quad + \mathbf{C}\ \mathbf{B}_{k+1}\ u_{MPC}(k+1), \\ \hat{y}(k+3) &= \mathbf{C}\ \mathbf{A}^3\ \mathbf{x}(k) + \mathbf{C}\ \mathbf{A}^2\ \mathbf{B}_k\ u_{MPC}(k) \\ &\quad + \mathbf{C}\ \mathbf{A}\ \mathbf{B}_{k+1}\ u_{MPC}(k+1) \\ &\quad + \mathbf{C}\ \mathbf{B}_{k+2}\ u_{MPC}(k+2),\ \text{etc.}\end{aligned} \tag{19}$$

It is straightforward to show that the following vector expression holds

$$\hat{\mathbf{Y}}(k) = \mathbf{G}\mathbf{x}(k) + \mathbf{F}\mathbf{U}(k), \tag{20}$$

with

$$\hat{\mathbf{Y}}(k) = \begin{bmatrix} \hat{y}(k+1) \\ \hat{y}(k+2) \\ \dots \\ \hat{y}(k+p) \end{bmatrix}, \quad \mathbf{U}(k) = \begin{bmatrix} u_{MPC}(k) \\ u_{MPC}(k+1) \\ \dots \\ u_{MPC}(k+p-1) \end{bmatrix} \tag{21}$$

and prediction horizon p. The system matrices for use in MPC result in

$$\mathbf{G} = \begin{bmatrix} \mathbf{C}\ \mathbf{A} & \mathbf{C}\ \mathbf{A}^2 & \dots & \mathbf{C}\ \mathbf{A}^p \end{bmatrix}^T, \tag{22}$$

$$\mathbf{F} = \begin{bmatrix} \mathbf{C}\mathbf{B}_k & \mathbf{0} & \dots & \mathbf{0} \\ \mathbf{C}\mathbf{A}\mathbf{B}_k & \mathbf{C}\mathbf{B}_{k+1} & \dots & \mathbf{0} \\ \dots & \dots & \dots & \dots \\ \mathbf{C}\mathbf{A}^{p-1}\mathbf{B}_k & \mathbf{C}\mathbf{A}^{p-2}\mathbf{B}_{k+1} & \dots & \mathbf{C}\mathbf{B}_{k+p-1} \end{bmatrix}, \tag{23}$$

where the prediction horizon p should not be chosen too large, considering that matrix $\mathbf{B}_k$ might change anytime. For $p = 2$, these matrices simplify to

$$\mathbf{G} = \begin{bmatrix} 1 \\ 1 \end{bmatrix}, \ \mathbf{F}(k) = -T_s \begin{bmatrix} \text{sign}(s(k)) & 0 \\ \text{sign}(s(k)) & \text{sign}(s(k+1)) \end{bmatrix}. \tag{24}$$

With given $\text{sign}(s(k))$, $\text{sign}(s(k+1))$ can be obtained from prediction (18) using the last step's β.

Problem 1: Given the system (20), find an optimal input $\beta(k)$ which minimizes the following cost function

$$\begin{aligned} J(k) = \frac{1}{2}\Big(\mathbf{Y}_d(k) - \hat{\mathbf{Y}}(k)\Big)^{\mathrm{T}} \mathbf{Q}\Big(\mathbf{Y}_d(k) - \hat{\mathbf{Y}}(k)\Big) \\ + \frac{1}{2}\mathbf{U}(k)^{\mathrm{T}}\mathbf{R}\mathbf{U}(k), \end{aligned} \tag{25}$$

where $\mathbf{Q}$ and $\mathbf{R}$ are non-negative definite matrices and $\mathbf{Y}_d(k)$ is the sliding surface reference trajectory for the next p time steps. In this case, its elements can simply be set to zero. The solution can be obtained in a closed form

$$\mathbf{U}(k) = (\mathbf{F}^{\mathrm{T}}\mathbf{Q}\mathbf{F} + \mathbf{R})^{-1}\mathbf{F}^{\mathrm{T}}\mathbf{Q}\big(\mathbf{Y}_d(k) - \mathbf{G}y(k)\big), \tag{26}$$

where $y(k) = s(k)$ and sliding mode control switching gain $\beta = \beta(k)$ is now chosen as the first element of $\mathbf{U}(k)$.

Remark 3: The MPC with the predicted sliding surface is realized with matrices (18) that do not depend on any systems parameters, and thus this approach states an intrinsic robustness of the prediction.

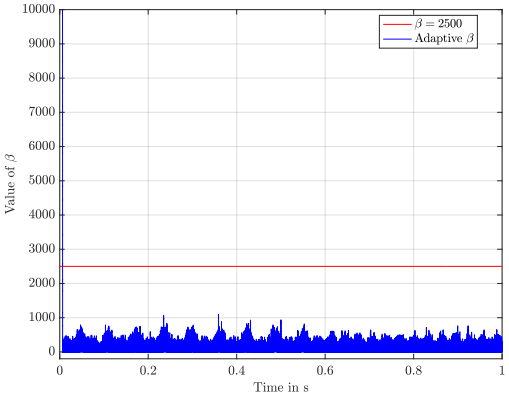

Fig. 3. Values of switching gain β for the scenario with sinusoidal load torques.

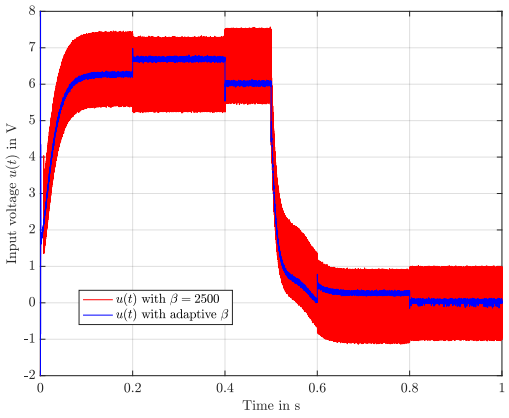

Fig. 4. Voltage $u(t)$ for pulsed load torques.

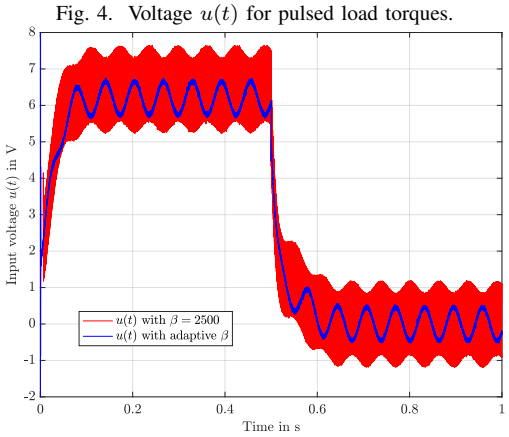

Fig. 5. Voltage $u(t)$ for sinusoidal load torques.

VI. Simulation Results

The simulations were performed using a number of practice-oriented artificial restrictions and loads. Namely, the motor input voltage $u(t)$ is restricted to [-12 V, 12 V]. The parameter T_{r0} for the Coulomb friction, which significantly influences the equivalent control part $i_{d_{eq}}(t)$, is biased with +20% error in the control law. Furthermore, additive white Gaussian noise with maximum amplitudes of 0.2% of the maximum of $\omega_d(t)$ is used in state feedback $\omega(t)$. The load torque, see $d(t)$ in (2), is modeled in two different scenarios – as a sine wave with

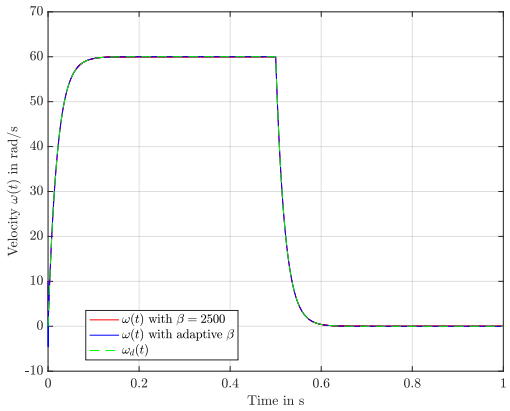

Fig. 6. Accurate tracking of $\omega_d(t)$ is achieved for all variants in both scenarios.

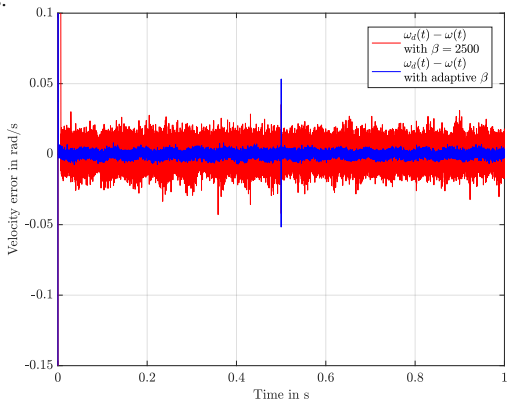

Fig. 7. Tracking error in the case of sinusoidal loads.

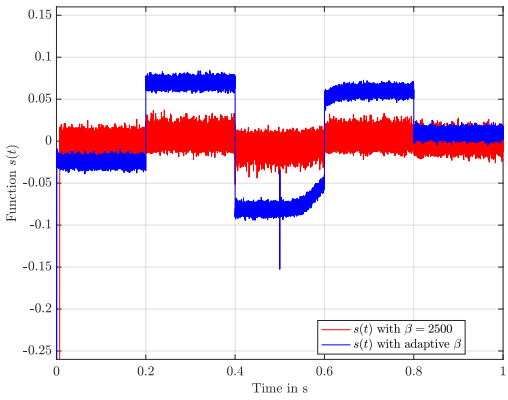

Fig. 8. Function $s(t)$ for pulsed loads.

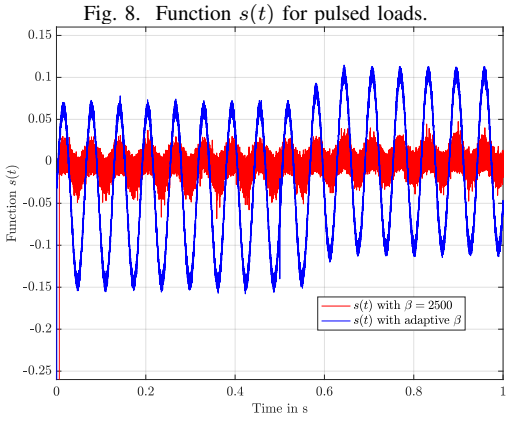

Fig. 9. Function $s(t)$ for sinusoidal loads.

an amplitude of 0.5 mNm and a frequency of 100 rad/s, and as a pulsed signal with random amplitudes within [-0.2 mNm, 5.5 mNm]. The control scheme of this simulation is shown in Fig. 2 where the loops can be retraced. Using this procedure, the chattering amplitude of the control input can be drastically reduced. This control strategy can be seen as an alternative to the well-known sliding surface thickness approach. In contrast to the latter, it can only reduce the chattering *amplitude* but not necessarily the frequency. However, the advantages make it worthwhile to conclude: The motion remains on the sliding surface because the necessary switchings according to the discontinuous term $\mathrm{sign}(s)$ are executed. The difference in chattering behavior for adaptive and constant values of β is shown in Fig. 3 up to Fig. 9. In Fig. 3, a comparison of magnitude w.r.t. a constant β and an adaptive $\beta(k)$ is depicted. Note that for sinusoidal loads $\beta(k)$ also shows a periodic behavior. The influence of different load characteristics can be seen best in Figs. 4 and 5 where the motor input voltages $u(t)$ are shown. It also demonstrates the significant reduction of the chattering amplitude because the control input signal is much smoother using the adaptive approach. Fig. 6 indicates at first glance that both controllers, with constant and adaptive β, are able to track the reference trajectory. However, when taking a closer look at the tracking error in Fig. 7, it can be stated that the adaptive approach works significantly better, as long as there are no discontinuities or too fast changes in the load or reference trajectory signals. Fig. 9 similarly shows residual oscillations in $s(t)$ even though the tracking error remains in the vicinity of zero. This large choice of α turned out to be necessary in simulations in order to ensure the cancellation of uncertain terms in the electrical subsystem (2). The superior performance of the adaptive variant, compared to the conventional SMC with a constant switching amplitude, can be seen in Table I, where the ITAE is defined as $\int |e(t)|t dt$ and the (input) energy is evaluated as $\int u^2(t) dt$. Note that the large differences in chattering amplitudes do not have much influence on the input energy computed this way. Figs. 10 to 13 show the results for another variant of the SMC based on the boundary layer approach, i.e., where $\mathrm{sat}(s)$ instead of $\mathrm{sign}(s)$ is used in the control law. An interesting effect can be observed in Fig. 8 ($s(t)$ for the adaptive variant) and in Fig. 10 ($s(t)$ for the boundary layer variant): Both show the behavior of $s(t)$ characterized by a nonzero value in several sections. In the latter case, this is caused by the permissible boundary region; nevertheless, the adaptive SMC shows a similar effect. As indicated in Table I, however, the adaptive approach performs comparably well compared to the boundary layer variant.

VII. Conclusions

To adaptively tune the switching gain of an SMC, a linear MPC scheme based on the closed-loop system dynamics is

TABLE I
MEASURES FOR THE TRACKING PERFORMANCE

	Const. β	**Const.** β **w/** sat	**Adaptive** β
ITAE	Sine ld.: 2.8 10^{-3} Pulse ld.: 2.7 10^{-3}	Sine ld.: 2.1 10^{-3} Pulse ld.: 4.4 10^{-4}	Sine ld.: 7.3 10^{-4} Pulse ld.: 6.9 10^{-4}
Energy	Sine ld.: 18.9 Pulse ld.: 20.1	Sine ld.: 18.2 Pulse ld.: 19.3	Sine ld.: 18.2 Pulse ld.: 19.3

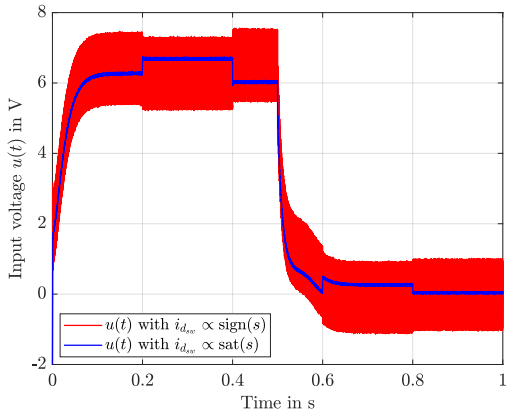

Fig. 10. Voltage $u(t)$ for pulsed load torques.

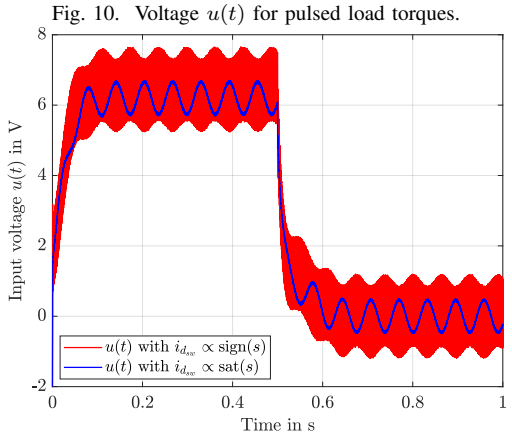

Fig. 11. Voltage $u(t)$ for sinusoidal load torques.

conceived. This strategy is applied to a DC drive in simulations in order to analyze its performance. This combination of an optimal and a robust controller is further extended using a flatness-based control to solve a velocity tracking problem. The simulations show great potential of this combination of controllers.

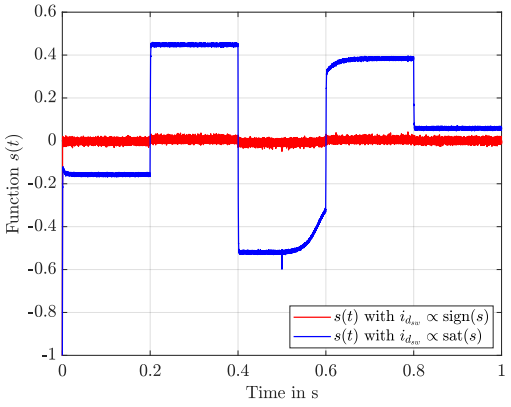

Fig. 12. Function $s(t)$ for pulsed loads.

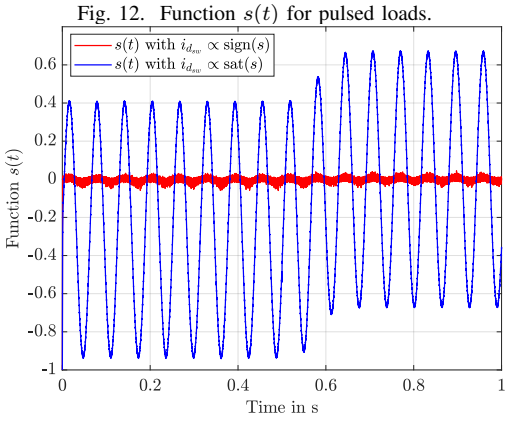

Fig. 13. Function $s(t)$ for sinusoidal loads.

REFERENCES

[1] Hyung-Tae Moon, Hyun-Soo Kim, and Myung-Joong Youn. A discrete-time predictive current control for PMSM. *IEEE Transactions on Power Electronics*, 18(1):464–472, Jan 2003.

[2] P. Mercorelli. Linear generalised model predictive control to avoid input saturation through matrix conditions. *WSEAS TRANSACTIONS on SYSTEMS*, 16:313–322, 2017.

[3] P. Mercorelli. A sufficient asymptotic stability condition in generalised model predictive control to avoid input saturation. In Klimis Ntalianis and Anca Croitoru, editors, *Applied Physics, System Science and Computers II*. Springer International Publishing, 2018.

[4] P. Kachroo and M. Tomizuka. Chattering reduction and error convergence in the sliding-mode control of a class of nonlinear systems. *IEEE Transactions on Automatic Control*, 41(7):1063–1068, Jul 1996.

[5] J. Liu, H. Li, and Y. Deng. Torque ripple minimization of PMSM based on robust ILC via adaptive sliding mode control. *IEEE Transactions on Power Electronics*, 33(4):3655–3671, April 2018.

[6] K. Jezernik, J. Korelič, and R. Horvat. PMSM sliding mode FPGA-based control for torque ripple reduction. *IEEE Transactions on Power Electronics*, 28(7):3549–3556, July 2013.

[7] C. Xia, G. Jiang, W. Chen, and T. Shi. Switching-gain adaptation current control for brushless DC motors. *IEEE Transactions on Industrial Electronics*, 63(4):2044–2052, April 2016.

[8] P. Mercorelli. A motion-sensorless control for intake valves in combustion engines. *IEEE Transactions on Industrial Electronics*, 64(4):3402–3412, April 2017.

[9] P. Mercorelli. A two-stage sliding-mode high-gain observer to reduce uncertainties and disturbances effects for sensorless control in automotive applications. *IEEE Transactions on Industrial Electronics*, 62(9):5929–5940, 2015.

[10] Brian Armstrong-Hélouvry, Pierre Dupont, and Carlos Canudas De Wit. A survey of models, analysis tools and compensation methods for the control of machines with friction. *Automatica*, 30(7):1083 – 1138, 1994.

[11] B. Haus, H. Aschemann, and P. Mercorelli. State estimation and second-order sliding mode control for a permanent magnet linear motor. In *Proc. of the 2018 American Control Conference*, Millwaukee (USA), June 2018.

[12] M. Fliess, J. Lévine, and P. Rouchon. Flatness and defect of non-linear systems: Introductory theory and examples. *International Journal of Control*, 61(6):1327–1361, 1995.

[13] M. J. Van Nieuwstadt and R. M. Murray. Real time trajectory generation for differentially flat systems. *International Journal of Robust and Nonlinear Control*, 8(11):995–1020, 1998.

[14] N. Faiz, S. Agrawal, and R. Murray. Trajectory planning of differentially flat systems with dynamics and inequalities. *J. Guidance, Control, and Dynamics*, 24(2):219–227, 2002.

[15] J.-J. E. Slotine and W. Li. *Applied nonlinear control*. Pearson, Upper Saddle River, NJ, 1991.